fMRI Head Motion as a Biomarker for Parkinson's Disease

Karan Singh
Department of Electrical Engineering
Stanford University
Stanford, CA 94305
karanps@stanford.edu

Kevin Liu
Department of Statistics
Stanford University
Stanford, CA 94305
liuxk@stanford.edu

Abstract

Head motion during resting-state fMRI is typically treated as a nuisance artifact, but emerging evidence suggests it may encode meaningful motor information relevant to neurodegenerative disease. In this study, we investigate whether raw head motion time series can be used to distinguish individuals with Parkinson's disease (PD) from healthy controls. Using framewise displacement data from the PPMI and HCP-Aging cohorts, we apply both classical and deep learning models to assess predictive signal in spontaneous motion patterns. Our approach includes an unsupervised Gaussian hidden Markov model (HMM) to uncover latent motion states, a supervised HMM-based classifier, and sequence-based deep learning models such as GRUs, LSTMs, and Transformers. We find that PD and control groups exhibit subtle but reproducible differences in temporal motion structure, with classification models achieving moderate accuracy and attention-based methods highlighting distinct patterns. These results suggest that head motion, though traditionally discarded, may offer a scalable and non-invasive biomarker for early PD detection. Code and data released at https://github.com/liuxk83/head-motion-analysis.

1 Introduction

Parkinson's disease (PD) is a progressive neurodegenerative disorder characterized by hallmark motor symptoms such as resting tremor, rigidity, and bradykinesia, as well as a range of non-motor symptoms that often precede diagnosis [8]. These early features—including hyposmia, constipation, and REM sleep behavior disorder—highlight the existence of a prolonged prodromal phase during which neurodegeneration progresses silently. However, PD diagnosis continues to rely primarily on observable clinical symptoms, which emerge late and vary substantially between individuals, limiting opportunities for early intervention.

At the same time, research into biological definitions of PD has advanced considerably, with growing interest in molecular markers such as α-synuclein and dopamine transporter loss [3]. Yet these gold-standard biomarkers remain invasive, expensive, and not easily scalable. As a result, there is a pressing need for accessible, non-invasive indicators that could flag PD earlier in its progression.

One underexplored source of signal is head motion during resting-state functional MRI (fMRI). Though typically treated as a nuisance variable and regressed out during preprocessing, head motion

39th Conference on Neural Information Processing Systems (NeurIPS 2025).

traces—captured through realignment parameters—may carry meaningful motor information. Subtle, disease-linked movements such as early tremor or instability could manifest in these sequences long before overt motor symptoms arise. Emerging evidence suggests that head motion is not merely random noise: summary motion metrics can distinguish between cognitive impairment and Alzheimer's disease [6], and individual-specific motion signatures have been found to correlate with behavioral traits.

Despite this promise, no large-scale study has assessed whether raw head motion time series can be used to detect PD or distinguish patients from controls. Furthermore, while sequence models such as hidden Markov models (HMMs) and recurrent neural networks have been successfully applied to behavioral and physiological time series in other domains [11], they remain largely untapped for analyzing fMRI-derived motion.

In this study, we investigate whether head motion patterns extracted from resting-state fMRI can serve as a discriminative signal for PD. We use data from the Parkinson's Progression Markers Initiative (PPMI), a large multi-site cohort comprising PD, prodromal, and healthy control participants with accompanying fMRI scans and motion traces. Our key questions are:

- Do head motion patterns differ reliably between PD patients and healthy controls?
- Can motion-derived features be used to classify PD with meaningful accuracy?
- Can unsupervised or interpretable models reveal structure in the motion signal that complements classification?

To answer these questions, we apply a combination of statistical preprocessing, hidden Markov models (HMMs), and deep learning classifiers—including GRUs, LSTMs, and Transformers—to raw head motion sequences. Our results demonstrate that head motion, despite being passively collected and typically discarded, may offer a promising signal for early-stage PD detection.

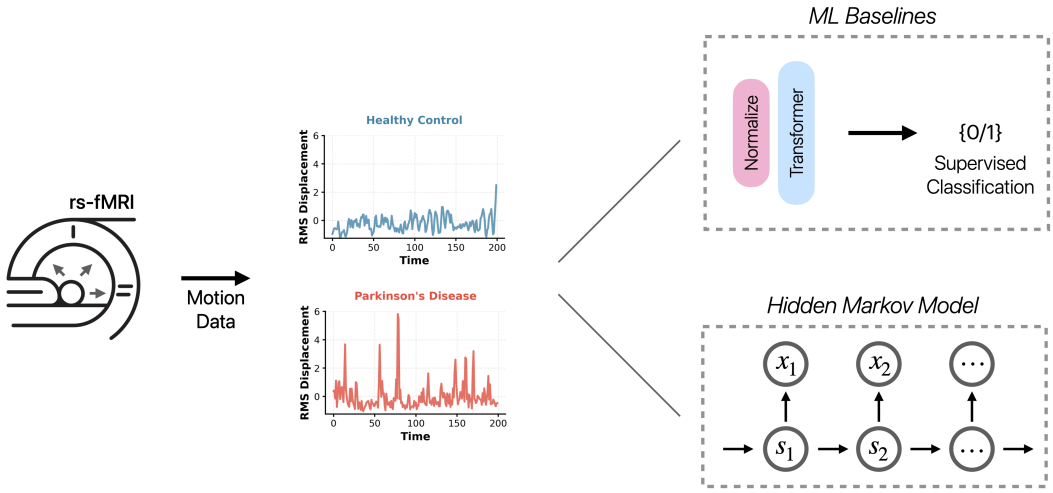

Figure 1: **Overview of our approach for detecting Parkinson's disease from resting-state fMRI-derived head motion.** Motion time series (e.g., RMS framewise-displacement) are extracted from resting-state fMRI scans of healthy control and Parkinson's disease subjects. These 1D sequences serve as input to two modeling pipelines: (top) supervised machine learning baselines, including a Transformer-based classifier following z-score normalization, and (bottom) an unsupervised hidden Markov model (HMM) to infer latent motion states and dynamics.

2 Related Work

Head motion in fMRI. Head motion during fMRI is typically treated as a nuisance artifact that degrades data quality, yet recent evidence suggests it may carry clinically meaningful signal. Haller et al. [6] found that simple motion metrics, such as global head rotation and axis-specific asymmetries,

differed systematically between healthy controls, patients with amnestic mild cognitive impairment (aMCI), and those with Alzheimer's disease (AD). These features achieved AUCs of 0.71–0.75 in distinguishing groups, suggesting that motion artifacts—normally discarded—may serve as useful biomarkers of neurodegeneration.

Further evidence from Bolton et al. [1] shows that even subtle, "clean" head motion contains subject-specific structure. In a large adult cohort, unsupervised clustering revealed reproducible subgroups of high- and low-motion individuals, with motion characteristics correlating with a range of anthropometric, cognitive, and neuropsychiatric traits—including anxiety, depression, and self-regulation. The authors emphasize that head motion carries structured, behaviorally relevant information, and caution against indiscriminate removal.

Head motion patterns in neurodegenerative disorders. These findings raise the question of whether neurological diseases systematically affect head motion. In Alzheimer's disease (AD) and related dementias, Haller et al. [6] found significantly elevated motion in patients compared to controls, potentially reflecting subtle motor impairment. Although motion is typically considered a confound in neuroimaging, its discriminatory power (AUC 0.7–0.75) suggests it may serve as a low-cost diagnostic signal.

For Parkinson's disease (PD)—a movement disorder—distinctive motion signatures might be expected. PD symptoms like tremor and bradykinesia could plausibly affect in-scanner motion, yet prior studies report weak or inconsistent group differences. For example, Liu et al. [7] observed no significant differences in mean head motion between early-stage PD patients and controls. Similarly, motion was not associated with freezing of gait or with clinical severity (UPDRS-III) in multi-site analyses [5]. These results suggest that simple summary metrics may miss subtler, disease-related motion patterns—perhaps due to compensatory akinesia or variable head tremor expression.

Crucially, the absence of mean-level differences does not rule out structured variation over time. Traditional metrics may be insensitive to transient behaviors like micro-tremor or positional instability. This motivates time-series modeling approaches that can capture temporal structure in motion data. To our knowledge, no prior work has attempted to classify PD vs. control using raw head motion sequences, despite evidence from Haller et al. [6] and Bolton et al. [1] that motion traces encode clinically relevant information.

Unsupervised sequence modeling offers a path forward. A prominent example is Motion Sequencing (MoSeq), introduced by Wiltschko et al. [11] to analyze animal behavior via autoregressive hidden Markov models (AR-HMMs). MoSeq learns a discrete "vocabulary" of motion motifs from 3D trajectory data and infers their probabilistic transitions. In mice, this approach outperformed traditional metrics in classifying drug exposures, and has since been applied to detect motor phenotypes in models of autism and Parkinsonism.

Applying HMMs to fMRI motion is a natural extension. These models capture not just how much a subject moves, but how motion evolves over time. Similar techniques have shown promise in human motor domains like gait and handwriting. In parallel, deep learning models such as Long Short-Term Memory (LSTM) networks have been used to classify PD from wearable sensors and voice data, learning temporal patterns like tremor frequency or speech irregularity. For example, Cuk et al. [4] achieved 87% accuracy in classifying early PD using an attention-augmented LSTM on gait time series. These results underscore the utility of both probabilistic and deep sequence models in extracting structured features from motion data.

Motion-derived features and clinical biomarkers. A key question is whether head motion features from fMRI relate to clinical or molecular markers of Parkinson's disease (PD). To date, no published study has linked motion dynamics to PD-specific biomarkers such as CSF α-synuclein or amyloid/tau, nor to prodromal indicators like REM sleep behavior disorder. Most neuroimaging work in PD focuses on functional connectivity or dopamine transporter imaging, with motion treated purely as a confound. One study did find that lower CSF α-synuclein was associated with disrupted connectivity, suggesting that imaging measures can reflect molecular pathology—though head motion was not analyzed [10]. In other disorders like ADHD and autism, higher in-scanner motion correlates with symptom severity, but similar analyses in PD have shown no association between mean motion and UPDRS scores. These findings suggest that coarse metrics may miss subtler, clinically relevant motion patterns. For instance, high-frequency tremor or postural instability could manifest as specific temporal signatures.

Whether individuals at risk for PD exhibit early motion anomalies also remains unexplored. Our study addresses this gap by examining whether motion-derived features can distinguish PD status in a large, multimodal dataset.

Our contributions. In summary, prior research indicates that head motion during fMRI is not merely an artifact but can carry diagnostic signals for neurological conditions. Small studies in Alzheimer's/MCI showed proof-of-concept that motion metrics distinguish patient groups [6], and large-sample analyses in healthy adults revealed that motion encodes stable person-specific information related to behavior and health [1]. However, there are several key gaps in the current literature that our work addresses:

- We evaluate whether raw head motion sequences—traditionally treated as noise—contain enough discriminative signal to classify PD vs. control. Using lightweight sequence models (GRUs, LSTMs, Transformers) and a supervised classifier based on HMMs, we benchmark predictive performance on standardized framewise displacement time series.
- Additionally, we apply hidden Markov models (HMMs) in an unsupervised fashion to discover latent motion "states" within the fMRI trace. This provides interpretable, structured descriptions of motion patterns and may capture transient behaviors (e.g., micro-tremors) missed by summary metrics.
- Lastly, for our transformer models, we extract and visualize self-attention maps to identify which timepoints contribute most to the classification decision. Like the HMM, this offers some insight into what motion signatures the model relies on, and how they differ across subjects.

3 Methods

3.1 Data Preprocessing

We analyze resting-state fMRI head motion traces from two sources: the Parkinson's Progression Markers Initiative (PPMI) [9] and the Human Connectome Project-Aging (HCP-Aging) datasets [2]. The PPMI dataset is a longitudinal, multi-site study comprising individuals with Parkinson's disease (PD), prodromal risk factors, and healthy controls, with standardized imaging protocols and extensive clinical characterization. Briefly, the imaging protocol incldues a repetition time (TR) of 2500 ms and approximately 240 timesteps (10 minutes) per run. Each subject underwent two runs with opposite phase-encoding directions (RL/LR). PD diagnosis is based on the UK Parkinson's Disease Society Brain Bank clinical criteria, including bradykinesia with either rest tremor or rigidity, confirmed by movement disorder specialists. Control subjects have no significant neurological diagnoses and show normal dopaminergic function on DaT-SPECT imaging.

The HCP-Aging dataset includes neurologically healthy adults aged 36–100, with resting-state fMRI acquired on Siemens 3T Connectom scanners, with a lower TR of 720ms and 420 timesteps (5 minutes) per run. Motion estimates are derived from a minimal preprocessing pipeline (specifically, fMRIPrep) and include framewise displacement averaged the volume, as a 1D timeseries, and the relative RMS displacement averaged over the volume.

From the PPMI and HCP datasets, we focus on a single time series: the root mean square deviation (RMSD) between successive frames. Our preprocessing pipeline consists of removing the first time point to eliminate baseline alignment artifacts, followed by z-score normalization per subject: $x_{\text{norm}} = \frac{x-\mu}{\sigma+\epsilon}$. Additionally, we remove any outliers, as measured by any samples with less than 100 timesteps, or with very low signal (a standard deviation below 1×10^{-6}). We end up with $N = 1809$ subjects in the processed data. Sequences are then are standardized to a fixed temporal length of 200 time points via zero-padding or truncation, producing uniform tensors of length $T = 200$.

For our ML methods, to harmonize the data distributions across the two datasets, we applied quantile matching between the control groups, mitigating scanner- or site-related differences. We confirmed that a classifier could not distinguish between control subjects across datasets post-harmonization, supporting the validity of this normalization. For all analyses, binary disease status (PD vs. control) serves as the classification label.

3.2 Modeling

We consider two broad categories of models for analyzing the data: models based on hidden Markov models (HMMs), and deep learning models.

3.2.1 HMM-Based Models

Unsupervised Model. Let $\mathbf{x}_i \in \mathbb{R}^T$ denote the RMSD for subject i, where $T = 200$ is the temporal length. To better understand the data, we first consider a Gaussian K-state HMM:

$$\begin{aligned} x_{i,t} &\sim \mathcal{N}\left(\mu_{z_{i,t}}, \sigma^2_{z_{i,t}}\right) && (t = 1, \ldots, T) \\ z_{i,t} &\sim \text{Cat}(\mathbf{P}_{z_{i,t-1}}) \\ z_{i,1} &\sim \text{Cat}(\boldsymbol{\pi}_0) \end{aligned}$$

where $z_{i,t} \in \{1, \ldots, K\}$ is the latent state associated with subject i at time t, $\mu_{z_{i,t}} \in \mathbb{R}^2$ and $\sigma^2_{z_{i,t}} \in \mathbb{R}^{2\times 2}$ are the parameters of the emission distribution, $\mathbf{P} \in [0,1]^{K\times K}$ is the transition matrix, and $\boldsymbol{\pi}_0 \in \Delta_K$ is the initial probability vector.

Training. We used the expectation-maximization algorithm to fit this HMM to the features $\{\mathbf{x}_i\}_{i=1}^N$. We determined the best number of components (states) through cross-validation. For each number of components $K \in \{2, 3, 4, 5, 6\}$, we fit three Gaussian HMMs as described above (using Python's `hmmlearn` package), each with different initializations and for $10K$ iterations (since convergence tends to be slower for larger K). We then took the HMMs with the lowest AICs of the three and constructed a plot of lowest AIC vs. K (see Figure 2). By heuristically looking for an "elbow" in this plot, we decided on $K = 3$ components for the Gaussian HMM. The best such HMM was then re-trained until convergence.

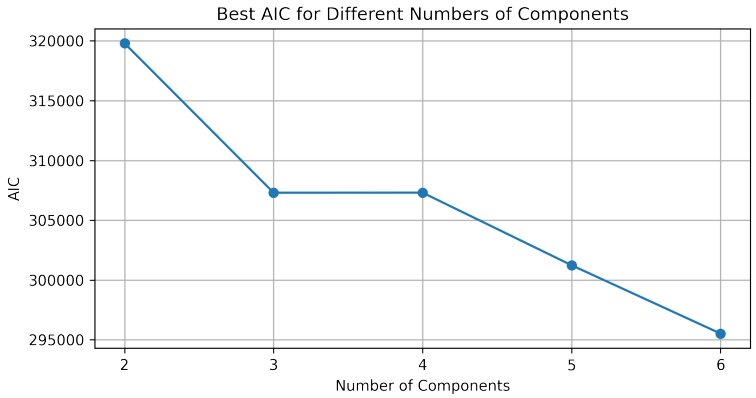

Figure 2: "Elbow plot" of lowest AIC (of the three initializations) vs. number of components K.)

Supervised Model. After fitting the 3-state Gaussian HMM, we analyzed the proportion of time spent by each subject in each state. (See Results section for more details.) These proportions could be predictors of disease status, so we were motivated to consider a variant of the model for supervised learning. Setting aside a random 20% of the original data as test data, we performed the same training process as described above, again choosing $K = 3$ components. We computed the proportion of time spent in each state as new features and used them in a logistic regression model to predict disease status.

3.2.2 Deep Learning

To assess whether motion traces from resting-state fMRI contain predictive signal for Parkinson's disease (PD), we trained several lightweight neural network classifiers using PyTorch. All models take as input the 1D root-mean-square (RMS) time-series displacement per subject.

Model Architectures. We evaluated both recurrent and transformer-based sequence models:

1. RNN-based models included GRU, LSTM, and vanilla RNN variants, implemented as single-layer recurrent cells with hidden dimension 64, followed by a fully connected layer to produce a binary logit.
2. Transformer models used a 2-layer encoder-only Transformer with 4 attention heads and embedding dimension d = 64. Input features were projected to this embedding space via a linear layer, with the final sequence representation obtained by global average pooling over the temporal dimension and passing the output to a fully connected output layer.

All models were trained using the PyTorch framework with the binary cross-entropy loss (BCEWithLogitsLoss) and the Adam optimizer. We used a learning rate of 1×10^{-3}, with a learning rate schedule defined by plateaus in the validation loss, which reduced the learning rate by a factor of 0.8 if the loss failed to improve for 200 consecutive epochs. Each model was trained for 50 epochs with a batch size of 32 on a single NVIDIA L40S GPU. Input sequences were z-score normalized per subject and padded or truncated to a uniform length of 200 time points. During training, we monitored validation accuracy, balanced accuracy, AUC, and loss to track convergence. All results are reported on a held-out validation set not used during training.

Additionally, to visualize how the transformer models attended to different parts of the motion sequence, we extracted attention weights from the final self-attention layer in the trained model. For each validation subject, we averaged the attention matrices across attention heads and across query positions to derive a single importance score per time point.

4 Results

4.1 Motion Patterns

After fitting the unsupervised Gaussian HMM, we predicted the most likely state sequences for each subject (Figure 3a) and computed statistics for each state (Table 1). In Figure 4, we also plot the distributions of the proportion of time spent in each state for both control and PD groups.

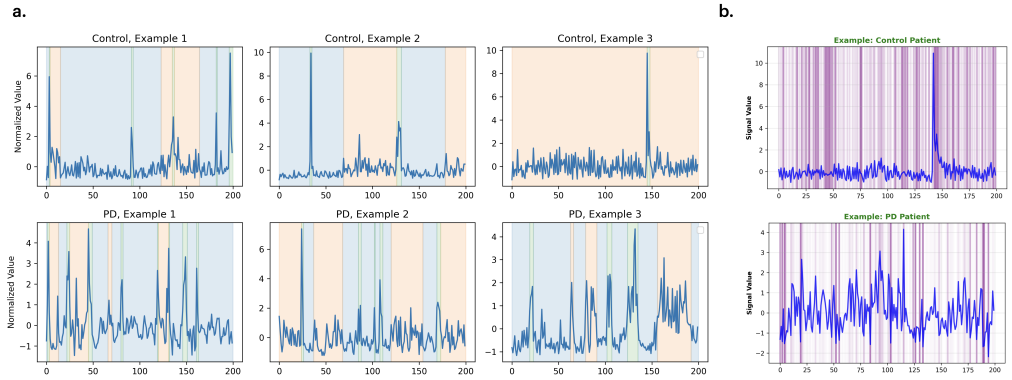

Figure 3: **a.** Distribution of proportions of time spent in each state for control and PD groups, for the HMM model. **b.** Visualization of the attention weights for an example control and PD patient. Attention weights are more distributed for the control patient, with no clear patterns, whereas the transformer appears to focus on spikes at more regular intervals in the head motion data from a Parkinson's patient.

Visually, we can see that the model has learned to classify peaks as their own state (shown in green in Figure 3). This corresponds to State 3 in Table 1, which has the highest mean and variance, as well as the lowest proportion of time for both groups.

On the other hand, the control and PD groups are subtly differentiated by the proportion of time spent in the other two states. PD subjects tended to spend more time in State 1, which is characterized by lower mean and variance. Meanwhile, control subjects tended to spend more time in State 2, which is

State	Mean RMSD	Variance of RMSD	Proportion of Time Spent in this State (Control)	Proportion of Time Spent in this State (PD)
1	-0.40	0.17	0.29	0.43
2	0.07	0.81	0.68	0.52
3	2.59	3.24	0.03	0.05

Table 1: Summary statistics for each state of the unsupervised Gaussian HMM.

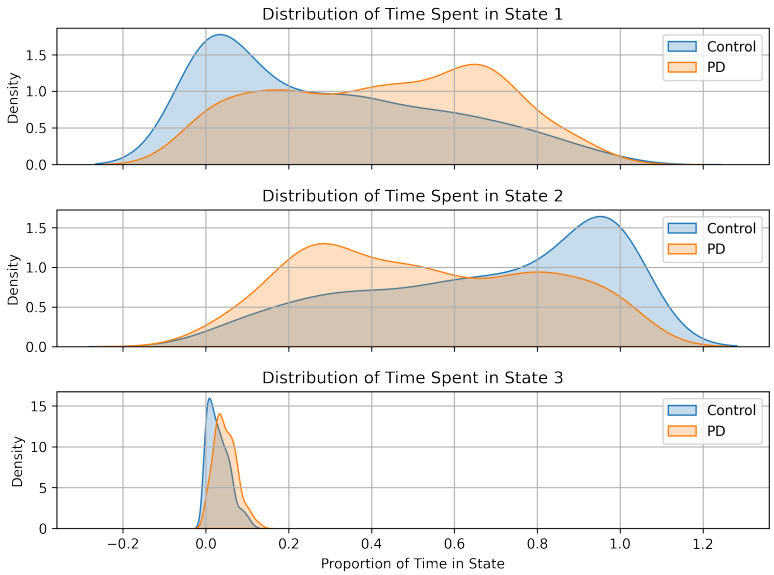

Figure 4: Distribution of proportions of time spent in each state for control and PD groups.

characterized by higher mean and variance. Thus, one might expect an RMSD graph for a control subject to be higher and more volatile than that for a PD subject.

4.2 Classification

The classification results from the various models we tested are summarized in Table 2.

Among the models tested, the Transformer achieved the most balanced performance, with near-equal sensitivity (0.65) and specificity (0.62), as well as the highest overall accuracy (0.66) and a competitive AUC of 0.67. In contrast, the GRU model reached the highest AUC (0.77) and specificity (0.95), but at the cost of much lower sensitivity (0.36), indicating a strong bias toward correctly identifying controls while missing many PD cases. The LSTM model showed generally weaker

	Specificity	Sensitivity	Accuracy	AUC
GRU	0.95	0.36	0.66	0.77
LSTM	0.77	0.41	0.59	0.55
Transformer	0.62	0.65	0.66	0.67
HMM	0.54	0.62	0.58	0.64

Table 2: Classification performance of sequence models on PD vs. control prediction from head motion. GRU achieves the highest AUC, while Transformer shows the best balance between sensitivity and specificity. HMM performs comparably, despite being unsupervised.

performance across all metrics. Interestingly, the unsupervised HMM-based classifier performed comparably to the deep models (AUC 0.64), suggesting that latent motion state dynamics alone carry meaningful discriminative signal.

5 Discussion

Conclusion. Our findings demonstrate that head motion traces extracted from resting-state fMRI scans – signals traditionally regarded as nuisance artifacts – contain subtle but reproducible patterns that differentiate individuals with Parkinson's disease from healthy controls. Using both interpretable statistical models and deep learning classifiers, we show that these motion-derived features offer modest but meaningful diagnostic signals. Notably, even simple models such as HMMs capture distinct temporal dynamics associated with PD, suggesting that underlying motor irregularities may be reflected in involuntary head movements during rest.

While our models do not yet achieve clinically actionable performance, they highlight a promising, low-cost, and non-invasive data source for detecting early motor changes associated with neurodegeneration. By treating motion as a signal rather than noise, this work opens the door to reusing widely available imaging data for secondary diagnostic purposes. Given the scalability and passive nature of motion tracking, such approaches could augment existing tools for screening or longitudinal monitoring, particularly in resource-limited or preclinical settings.

Limitations. This study has a few limitations that should be considered. For example, the data are imbalanced, with more HCP controls than PD subjects (from PPMI) and more PD subjects than PPMI controls, which may bias classification performance. Also, potential confounds such as scanner site, age, sex, and head size may also influence motion patterns despite standard harmonization efforts. Moreover, our analysis was limited to resting-state fMRI, lacking the behavioral context of task-based paradigms, and did not include longitudinal or multimodal data that could improve prediction or interpretability. Finally, while both HMM and deep learning models show promise, they may oversimplify the temporal complexity of PD-related motion or overfit without sufficient regularization and validation.

Future Work. Future efforts will focus on improving data quality and consistency, as well as model robustness or interpretability. For example, extending our models to incorporate longitudinal data could help track disease progression or predict conversion in at-risk individuals. Integration with task-based fMRI or wearable sensor data may enhance signal quality and context specificity. To support clinical adoption, we could also validate our approach in prospective cohorts and explore real-time motion analytics during routine imaging workflows.

From a modeling perspective, richer probabilistic frameworks – such as switching linear dynamical systems or hierarchical HMMs – could capture finer-grained motion states and transitions. In addition, besides using HMMs for supervised and unsupervised learning, we could also explore *semi-supervised learning* frameworks, such as learning group-specific HMMs that may share the same states and emissions but have different transition matrices.

Together, these directions could lead to more generalizable, interpretable, and clinically actionable models of brain dynamics in Parkinson's disease.

References

[1] Thomas A.W. Bolton, Valeria Kebets, Enrico Glerean, Daniela Zöller, Jingwei Li, B.T. Thomas Yeo, César Caballero-Gaudes, and Dimitri Van De Ville. Agito ergo sum: Correlates of spatio-temporal motion characteristics during fMRI. *NeuroImage*, 209:116433, 4 2020. ISSN 10538119. doi: 10.1016/j.neuroimage.2019.116433.

[2] Susan Y. Bookheimer, David H. Salat, Melissa Terpstra, Beau M. Ances, Deanna M. Barch, Randy L. Buckner, Gregory C. Burgess, Sandra W. Curtiss, Mirella Diaz-Santos, Jennifer Stine Elam, Bruce Fischl, Douglas N. Greve, Hannah A. Hagy, Michael P. Harms, Olivia M. Hatch, Trey Hedden, Cynthia Hodge, Kevin C. Japardi, Taylor P. Kuhn, Timothy K. Ly, Stephen M. Smith, Leah H. Somerville, Kâmil Uğurbil, Andre van der Kouwe, David Van Essen, Roger P.

Woods, and Essa Yacoub. The Lifespan Human Connectome Project in Aging: An overview. *NeuroImage*, 185:335–348, 1 2019. ISSN 10538119. doi: 10.1016/j.neuroimage.2018.10.009.

[3] Lana M. Chahine, Kalpana Merchant, Andrew Siderowf, Todd Sherer, Caroline Tanner, Kenneth Marek, and Tanya Simuni. Proposal for a Biologic Staging System of Parkinson's Disease. *Journal of Parkinson's Disease*, 13(3):297–309, 3 2023. ISSN 1877-7171. doi: 10.3233/JPD-225111.

[4] Aleksa Cuk, Timea Bezdan, Luka Jovanovic, Milos Antonijevic, Milos Stankovic, Vladimir Simic, Miodrag Zivkovic, and Nebojsa Bacanin. Tuning attention based long-short term memory neural networks for Parkinson's disease detection using modified metaheuristics. *Scientific Reports*, 14(1):4309, 2 2024. ISSN 2045-2322. doi: 10.1038/s41598-024-54680-y.

[5] Christopher G. Goetz, Barbara C. Tilley, Stephanie R. Shaftman, Glenn T. Stebbins, Stanley Fahn, Pablo Martinez-Martin, Werner Poewe, Cristina Sampaio, Matthew B. Stern, Richard Dodel, Bruno Dubois, Robert Holloway, Joseph Jankovic, Jaime Kulisevsky, Anthony E. Lang, Andrew Lees, Sue Leurgans, Peter A. LeWitt, David Nyenhuis, C. Warren Olanow, Olivier Rascol, Anette Schrag, Jeanne A. Teresi, Jacobus J. van Hilten, and Nancy LaPelle. Movement Disorder Society-sponsored revision of the Unified Parkinson's Disease Rating Scale (MDS-UPDRS): Scale presentation and clinimetric testing results. *Movement Disorders*, 23(15): 2129–2170, 11 2008. ISSN 0885-3185. doi: 10.1002/mds.22340.

[6] Sven Haller, Andreas U. Monsch, Jonas Richiardi, Frederik Barkhof, Reto W. Kressig, and Ernst W. Radue. Head Motion Parameters in fMRI Differ Between Patients with Mild Cognitive Impairment and Alzheimer Disease Versus Elderly Control Subjects. *Brain Topography*, 27(6): 801–807, 11 2014. ISSN 0896-0267. doi: 10.1007/s10548-014-0358-6.

[7] Yanjun Liu, Mengyan Li, Haobo Chen, Xinhua Wei, Guihe Hu, Shaode Yu, Xiuhang Ruan, Jin Zhou, Xiaoping Pan, Ze Li, Zhenhang Luo, and Yaoqin Xie. Alterations of Regional Homogeneity in Parkinson's Disease Patients With Freezing of Gait: A Resting-State fMRI Study. *Frontiers in Aging Neuroscience*, 11, 10 2019. ISSN 1663-4365. doi: 10.3389/fnagi.2019.00276.

[8] Philipp Mahlknecht, Klaus Seppi, and Werner Poewe. The Concept of Prodromal Parkinson's Disease. *Journal of Parkinson's Disease*, 5(4):681–697, 10 2015. ISSN 18777171. doi: 10.3233/JPD-150685.

[9] Kenneth Marek, Sohini Chowdhury, Andrew Siderowf, Shirley Lasch, Christopher S. Coffey, Chelsea Caspell-Garcia, Tanya Simuni, Danna Jennings, Caroline M. Tanner, John Q. Trojanowski, Leslie M. Shaw, John Seibyl, Norbert Schuff, Andrew Singleton, Karl Kieburtz, Arthur W. Toga, Brit Mollenhauer, Doug Galasko, Lana M. Chahine, Daniel Weintraub, Tatiana Foroud, Duygu Tosun-Turgut, Kathleen Poston, Vanessa Arnedo, Mark Frasier, and Todd Sherer. The Parkinson's progression markers initiative (PPMI) – establishing a PD biomarker cohort. *Annals of Clinical and Translational Neurology*, 5(12):1460–1477, 12 2018. ISSN 2328-9503. doi: 10.1002/acn3.644.

[10] Xuyang Wang, Kwangsun Yoo, Huafu Chen, Ting Zou, Hongyu Wang, Qing Gao, Li Meng, Xiaofei Hu, and Rong Li. Antagonistic network signature of motor function in Parkinson's disease revealed by connectome-based predictive modeling. *npj Parkinson's Disease*, 8(1):49, 4 2022. ISSN 2373-8057. doi: 10.1038/s41531-022-00315-w.

[11] Alexander B. Wiltschko, Tatsuya Tsukahara, Ayman Zeine, Rockwell Anyoha, Winthrop F. Gillis, Jeffrey E. Markowitz, Ralph E. Peterson, Jesse Katon, Matthew J. Johnson, and Sandeep Robert Datta. Revealing the structure of pharmacobehavioral space through motion sequencing. *Nature Neuroscience*, 23(11):1433–1443, 11 2020. ISSN 1097-6256. doi: 10.1038/s41593-020-00706-3.